Desalination and Water Treatment
www.deswater.com

12 (2009) 169–184

1944-3994 / 1944-3986
doi: 10.5004/dwt.2009.919

Less polluting and more affordable future desalination

Y.M. El-Sayed

Advanced Energy Analysis, 41658 Higgins Way, Fremont, CA 94539, USA
Tel. +1 (510) 657-7423; Fax +1 (510) 656-2783; email aea87@comcast.net

Received 24 September 2009; Accepted 30 September 2009

ABSTRACT

The systems of nine desalination configurations are analyzed for efficiency, cost and polluting effects to map a road towards the most fit future desalination systems as well as research and development programs related to their advancement. The motive for this analysis is the rising consumption of apparently depleting fossil fuel resources and their associated rising emissions. The configurations are presented. The methodology of analysis is briefly described and the methodology details are referenced. The relevant results are summarized. The effects of variable power demand and variable oil price index are evaluated. Power-driven desalination processes run independently by efficient fuel-driven prime movers where renewable energy resources are absent and power-driven membrane desalination processes run by photovoltaic solar cells where the sun shines are likely to gain popularity. The load factor of a power plant of a variable power demand is improved by running a desirable power-driven night product in demand. Zero liquid discharge desalination requires more basic research.

Keywords: Thermal and membrane desalination; Fossil fuel driven and solar-power driven desalination; CO_2 emission; Zero liquid discharge; Changing oil prices; Variable-power/constant water production and night product

1. Introduction

Any production system, including desalination, requires fueling. The system is also embedded in two main environments: the physical environment and the economic environment.

As for fueling, desalted water may be directly or indirectly fossil-fuel-driven, nuclear-fuel-driven or renewable-energy-driven. It is indirectly driven when co-produced with electric power or driven by grid power.

When desalted water is co-produced with electric power, the combination of the variable power demand and the steady water production has a profound negative effect on system overall efficiency.

When desalted water is fossil-fuel-driven directly or indirectly, two streams are to be dumped in the physical environment: an exhaust gas stream and a brine stream of elevated salt content. When the exhaust is dumped in air, CO_2 emission occurs. When concentrated brine is dumped back in the sea, harm is done to marine life and when dumped back in underground, the salinity of the underground water rises at a rate depending on the size of underground water. Dumping waste directly in the physical environment is the cheapest way to get rid of the waste at the expense of the environment.

When desalted water is solar, wind or tide driven, only the brine stream needs dumping. Exhaust gases are absent as well as CO_2 emission. This makes renewable energy-driven-desalination systems in the lead of being friendly with the physical environment in regard to CO_2 emission.

For fossil-fuel-driven desalination systems, the higher the efficiency of the system, the lower is the fuel burning and hence the CO_2 emission for the same produced product or products, until cost looses its competitiveness in the market and sets a limit to the reduction of CO_2 emission. The economic environment imposes the limit.

The economic environment is not anymore steady. The concern of depleting fuel resources causes fluctuations in world oil prices. The polluting effect of fuel burning raises an environmental concern.

In view of the above, a number of different desalination configurations will be evaluated in terms of efficiency, cost and polluting effects. The CO_2 emission is first considered assuming that the direct dumping of concentrated brine is tolerated.

The avoidance of direct brine dumping is treated by going to zero liquid discharge where more desalted water is obtained and the safe dumping of solid salts becomes manageable by transport to safe dumping locations. Pre-dumping treatment is another option to safe dumping. The idea of generating power by the concentration difference of rejected brine and its feed while reducing the concentration of the rejected brine is another option. None of these dumping options is economic so far.

2. The systems analyzed

Systems of nine desalination configurations are considered. Six configuration types are fossil-fuel-driven burning natural gas, two are solar-driven and one is concentrated-brine-driven. Figs. 1–9 show the flow diagrams of the nine configurations and their references are indicated.

Each flow diagram is identified by its basic devices (in bold numbers) their inlet and exit streams (in un-bold numbers).

2.1. The methodology of analysis

The methodology of analysis starts first as an exergy-based simple thermodynamic analysis. Each configuration has its working fluids and the data for their thermodynamic and transport properties and its selected thermodynamic decision variables. The decision variables are mostly efficiency parameters along with few pressure and temperature levels. They are selected to reach a feasible design point fast by the most direct computational path with least iteration loops while satisfying mass balance, energy balance and exergy balance equations. A thermodynamic design point has each stream state computed (pressure, temperature, specific volume, enthalpy, entropy, exergy, and composition) and has each device process computed (mass rates, heat rate, power, exergy destruction). An overall energy balance and exergy balance verify the consistency of the computed design point. Thus far costs are absent.

To extend the methodology for analysis to handle cost, a characterizing surface of heat transfer (e.g. for heat exchangers), of mass transfer (e.g. for membranes) or of momentum transfer (e.g. for blades) is identified of each device. Design models are invoked to compute a device surface for its given efficiency parameters (or minimized surface if design degrees of freedom exist). The cost of the device is rated per unit manufacturing cost of the characterizing surface. Manufacture models (or empirical formulae in the absence of models since manufacture models are less developed than design models) are invoked to compute the surface unit cost. The cost of making a device is now computed. The cost of fueling a device is the cost of its exergy destruction. Introducing a system single exergy destruction price, the cost of fueling a device is obtained. Now the making and fueling costs of a device can be balanced for minimum device cost by changing the thermodynamic decision variables of the device. The fast system computation enhances the optimization of a configuration for lower production cost. The methodology is step-by-step detailed in reference [1]. The justifications of the simplifying assumptions of device-by-device cost minimization and the use of a system unit cost of exergy destruction are explained.

The results of the computations are presented in tables of states, processes and costs. Only the highlights of results are given in this paper

The purpose of the computations is to capture ideas that may help meeting the challenges of depleting fossil-fuel resources and increased CO_2 emissions as well as the harm of dumped waste.

2.2. The flow diagrams of the configurations

The similarities and differences among the flow diagrams of the nine configurations, Figs. 1–9, are first described followed by the major features and results of each.

Each of the nine configurations has two design points: a reference design point and an improved design point by automated or manual optimization. For the systems of configurations 1 and 2 the improved design point is obtained by automated optimization. The design models of their devices offer more than one surface for a given performance (design degrees of freedom exist). For the rest of the configurations, the design degrees of freedom are quite limited. The improved design point is sought by manually changing the thermodynamic decision variables intuitively.

Two economic environments are also considered. One represents a default oil index price of $25/barrel (default) and one represents $100/barrel. Although it is difficult to predict the price structure under different oil price indices, a simple prediction is considered. Fuel, power and steam costs at the economy of $100/barrel are set at 4 times those at $25/barrel. The unit surface manufacture costs of devices and the costs of products are set at a lower rate of 2 times.

The GT/MSF configuration has two products (power and water) while being driven by a single fuel resource. Often, the decision variables of the system permit one product rate as a decision variable. Power of 100 MW is selected as the decision product rate. The objective of maximizing profitability is considered for this particular configuration. Computed water product rates ranged from 8 to 10 migd.

For cogeneration systems in general, various assumptions have been proposed to allocate the production cost to water and power. The assumptions are all logical but the allocations differ significantly. The allocation assumed here considers the capital cost of each subsystem as belonging to the subsystem. The fuel is allocated in proportion to the exergy destructions of devices and the exergy of waste streams of each subsystem. This gives a lower bound to the cost of water since no devices or their exergy destructions are shared by the two subsystems. Higher water cost is obtained if, for example, the exergy destruction of combustion is shared.

For the GT/MSF and SCC systems, a default power load profile that varies from 20 to 100 MW of load factor 0.583 is assumed. Ideal and actual control features are considered. Ideal control assumes design efficiency at all load fractions (implying variable geometry devices). The actual control considered keeps the air rate to the gas turbine compressor at design value while reducing the fuel/air ratio. For the GT/MSF systems, re-firing at the exit of the gas turbine maintain constant steam to the MSF. For the SCC, the steam to the steam turbine and the cooling water to the condenser are controlled by water-level indicators in boiler and condenser.

A quadratic equation for power/fuel efficiency as function of load fraction is assumed to obtain the fuel consumption profile under variable power demand. The considered quadratic equation assumes design efficiency at maximum load and 20% the design efficiency (default) at a minimum load fraction of 0.2. The efficiency assigned to the 0.2 load fraction decides the variable load efficiency profile. Both GT/MSF and SCC systems are run without and with night products to evaluate the effects of improved load factor. Both systems considered RO subsystem for the night product. Two time periods are identified for the default load profile. The first starts from midnight to 6 am where a power of 80±5 MW is available. The second starts from 7 pm to 11 pm where a power of 40 MW±5 MW is available. For the SCC system, a water electrolysis subsystem [13,14] producing H_2 and O_2 as night products is also considered.

For the SCC-driven VC and RO desalting systems, two types of the rejected stream disposal are assumed: a conventional brine discharge and salt discharge (zero liquid discharge).

For the PV/RO and PV/ED solar systems, a solar intensity profile at 30° north latitude is assumed.

Solar thermal desalination systems such as solar stills and multiple effect distillation driven by evacuated tube collector [3] are not considered because of their high thermal solar collection cost and low water separation efficiency and hence high unit water product cost. Cost of product water as high as 6 $/m^3 has been reported.

For the osmosis power systems (tapping power from two streams of different salt concentrations), sodium chloride ideal solution is assumed. Salt content 0.035 is assumed for seawater and up to 0.25 salt content is assumed for the driving brine.

For systems of Figs. 1–6 the imperial gallon happened to be used for desalination sizing. For systems of Figs. 7–9, the US gallon happened to be used. The imperial gallon is 1.2 the US gallon.

All systems assume a relatively abundant feed resource for saline water. Zero chemical exergy is assigned to the feed resource. Changing the salt content of the feed resource automatically assigns zero chemical exergy to the new value. In the absence of detailed composition of the feed resource, the properties of sodium chloride solutions are assumed.

2.2.1. The GT/MSF configuration of 100 MW power [1]

- The configuration represents a gas turbine power and a multistage flash seawater distillation co-generating power and distilled water
- The configuration has 46 states, 22 devices and 68 thermodynamic decision variables of which 24 are manipulated for improved designs.
- The gas turbine compressor delivery pressure is set at 135 psia. Firing temperature is set low at 1600 F to avoid gas-turbine-blade cooling, though blade cooling is allowed for. Steam is generated at 240 psia and 450 F and throttled to drive the MSF. Seawater feed of 0.035 salt content is assumed and reject brine is set to 0.07 salt content.
- A night product raises the load factor from 0.583 to 0.867 and produces 5667 t/h desalted water <500 ppm assuming RO power requirement 5 kWh/t and surface requirement 20 m^2/(t/h). Profitability is reduced in the absence of a night product and is raised 5–10 times the design steady state value in the presence of a night product, assuming all night product is saleable.
- The CO_2 emission is slightly reduced from 64 t/h to 56 t/h with improved design since burning fuel by re-firing is essential to maintain the steady production of the MSF distiller. Auxiliary boilers and the throttling of high pressure steam are alternatives that maintain the steady production of MSF distiller with the same weak effect of reducing CO_2 emission
- Automated optimization changed all the 24 manipulated decision variables. For example, the number of

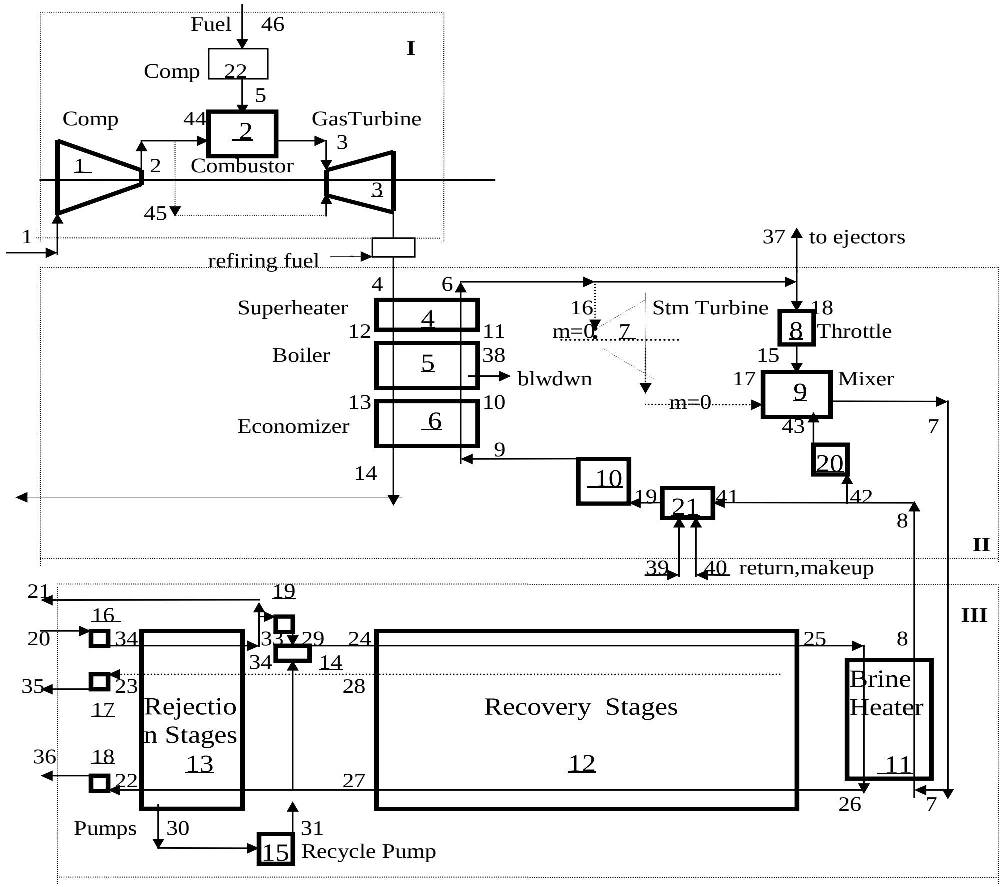

Fig. 1. GT/MSF co-generation system [1].

MSF stages is raised for its reference design value of 18 to 28, the pinch point is reduced from 50 F to around 10 F and the adiabatic efficiencies of compressor and gas turbine are raised from 0.84 and 0.9 to 92 and 0.921 for higher profitability.

- The improved design point is different under each of the two considered economies of $25 and $100/barrel oil.
- The fuel penalty of actual control compared to ideal control (the design efficiency remains constant at all load fractions) for the reference system is 97 MW with no night product.

2.2.2. The SCC configuration of 100 MW power [1]

- The configuration represents a simple combined cycle (one boiler pressure).
- The configuration has 20 states, 11 devices, 34 thermodynamic decisions of which 18 are manipulated for improved designs.
- The compressor delivery pressure is set at 135 psia. Firing temperature is set at 1600 F. Steam pressure is set at 600 psia.
- A night product raises the load factor from 0.583 to 0.867 and produces 5667 t/h desalted water <500 ppm when installing a night RO desalter of currently attainable power requirement of 5 kWh/t and surface requirement 20 m^2/(t/h). A night product also produces 0.349 t/h H_2 and 2.798 t/h O_2 (consuming 3.148 H_2O) when installing a night water electrolyzer of power requirement 78.25 MWh/t H_2 which is ΔG_f of water divided by an efficiency of 0.42 for a direct current intensity of 1 A/cm^2 [13,14]
- Profitability is reduced or becomes a loss in the absence of night products and is raised 5 to 10 times the design steady state value in the presence of night products, provided all night products are saleable.
- The CO_2 emission design value is 45 t/h (compared to 64 t/h of the GT/MSF case). The emission is reduced to 40 t/h with improved lower production cost.
- The fuel penalty of actual control compared to ideal control is 69 MW with no night product and is reduced to 14 MW with night water product. For oxygen and hydrogen night production, the fuel penalty is as high as 245 MW and is reduced to 224 MW with improved design.

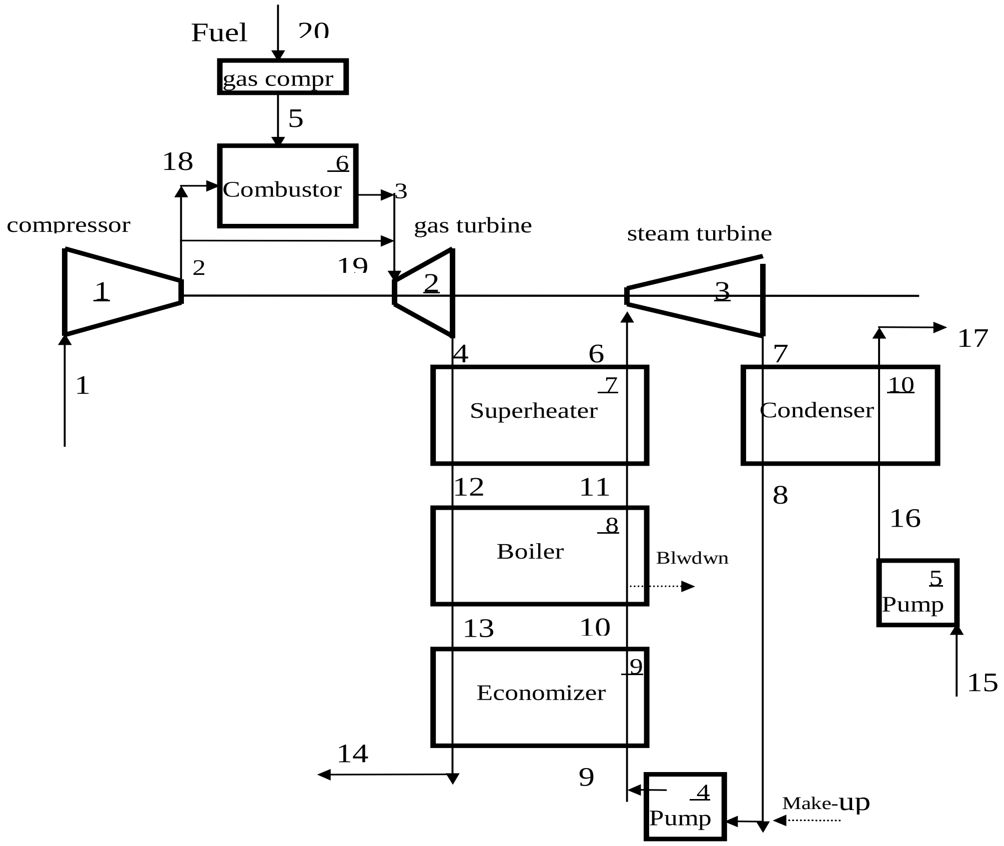

Fig. 2. Simple combined cycle (SCC) [1].

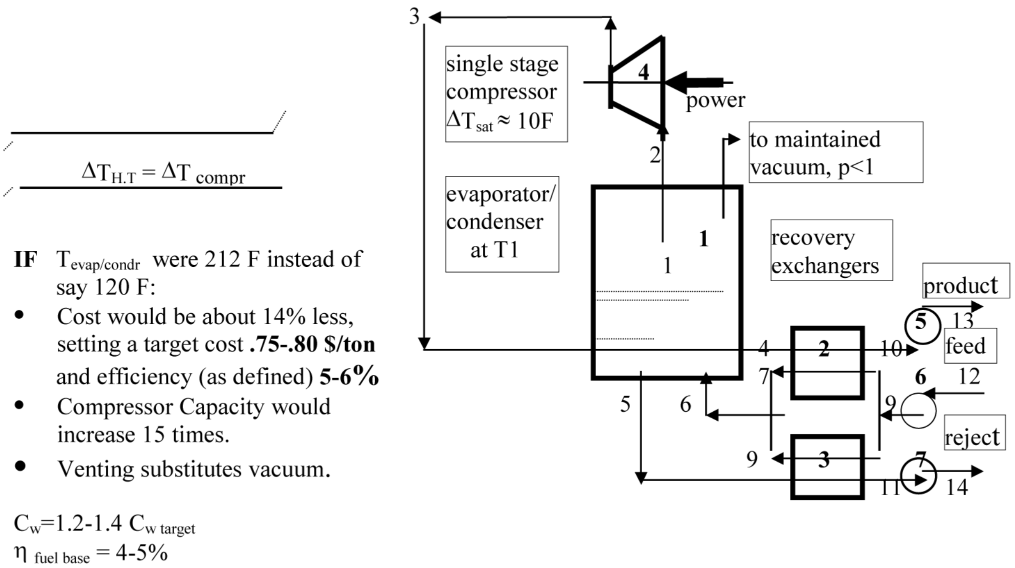

Fig. 3. Vapor compression distiller (VC) [1].

2.2.3. SCC/VC configuration of 10 migd product water [1]

- Fig. 3 represents a vapor compression seawater distiller VC producing only water. The VC is driven by a simple combined cycle having the configuration of Fig. 2.
- The vapor compression distiller VC has 14 states, 7 devices and 18 thermodynamic decisions of which 3 are manipulated for improved designs.

- No night product is introduced because the production is a steady state production of 10 migd water by VC desalter
- The combined cycle subsystem of the SCC/VC combination minimizes its production cost given the power called for by the vapor compression subsystem and the fuel price set by the considered economy. This establishes the unit cost of power to vapor compression subsystem as an internal power price.
- The reference design of the VC distiller has a capital cost 34.6 M$ for compressor and heat exchange surfaces and requires 46 MW power. The driving simple combined cycle requires in turn 114 MW fuel. The improved SCC design for lower production cost has these 3 numbers 217 M$, 19 MW power and 43 MW respectively.

2.2.4. SCC/VC ZLD configuration of 10 migd product water

- The configuration is similar to Fig. 3 but the vapor compression distiller is modified for zero liquid discharge.
- The VC ZLD of Fig. 4 has 16 states, 10 devices and 19 thermodynamic decisions of which none is manipulated.
- The concept of zero liquid discharge is considered using single stage VC. The result, so far, is not cost effective. Power requirement of the reference case of zero liquid discharge is more than double that of brine discharge so is the CO_2 emission. For the improved design case by lower SCC cost, the power and emission are almost 4 times those of the brine discharge. The unit cost of water almost tripled. In all the runs of the zero liquid discharge case, the profitability of the SCC/VC ZLD combination is a loss. Although the high-pressure requirement of the SCC/RO systems is avoided, large parallel compressors operating under vacuum are needed.

2.2.5. SCC/RO configuration of 10 migd product water

- The configuration represents a reverse osmosis seawater desalter RO producing only water. The RO is driven by a simple combined cycle having the configuration of Fig. 2.
- The one stage RO desalter [2,4,5] has 10 states, 3 devices and 18 thermodynamic decisions of which 12 are

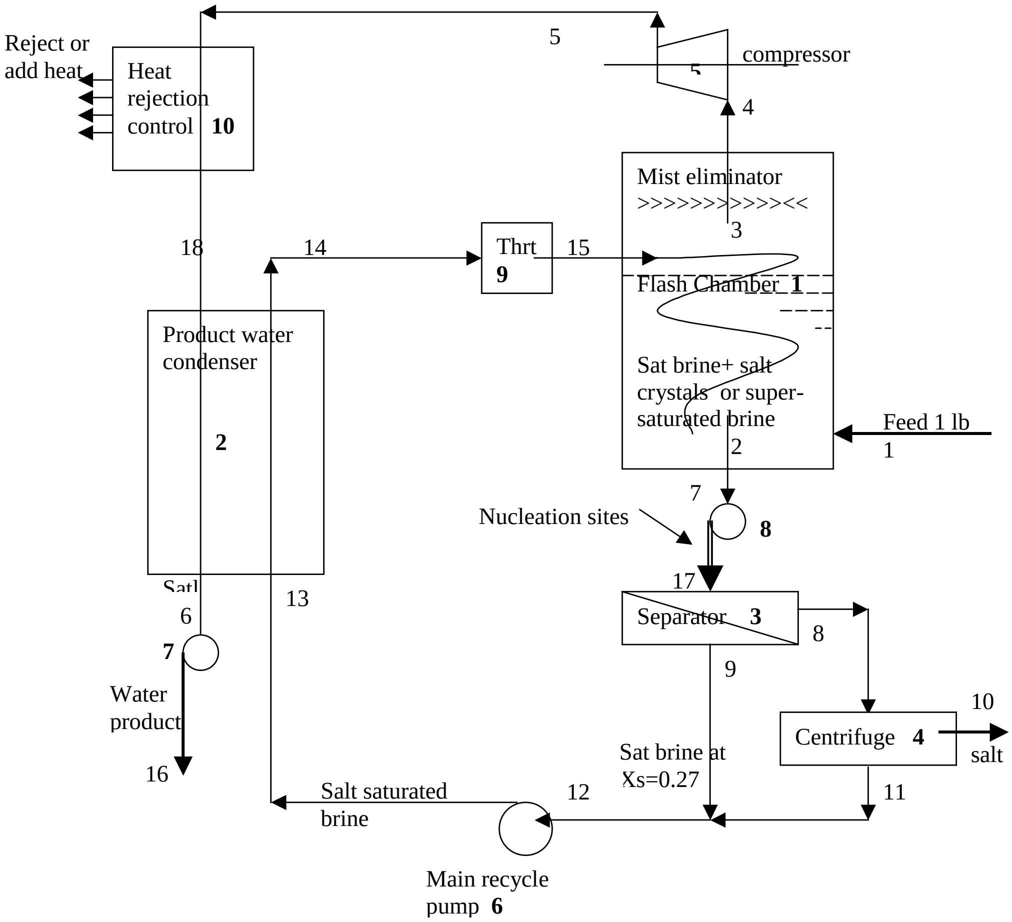

Fig. 4. VC for zero liquid discharge (ZLD).

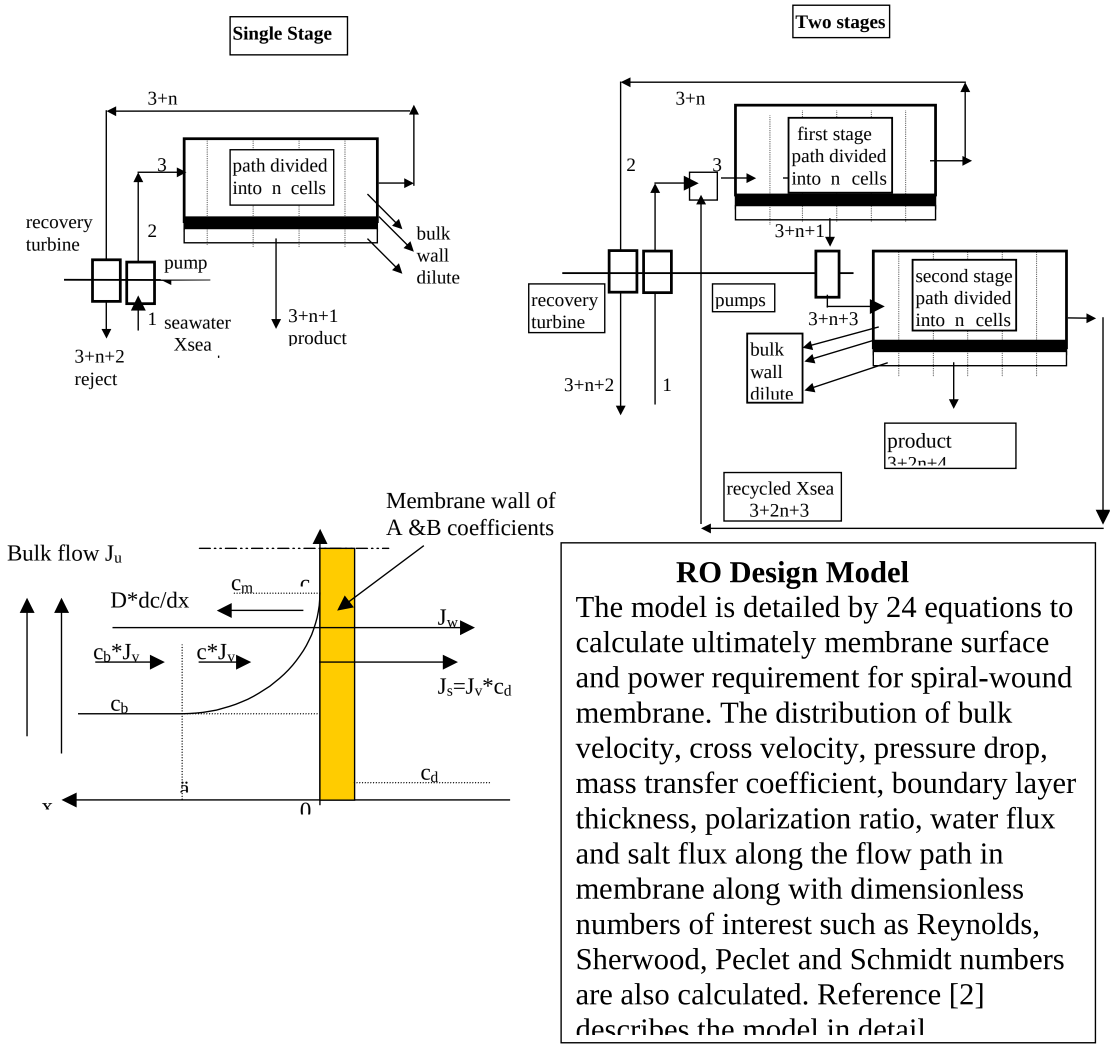

Fig. 5. The reverse osmosis desalter (RO) [1,2].

manipulated for improved designs. The two-stage system is a standby system in case the one stage fails to deliver the drinkable quality of the product water.

- No night product is introduced because the production is a steady state production of 10 migd water by RO desalter
- The combined cycle subsystem supplies the power called for by the RO subsystem and minimizes the production cost of combined cycle subsystem using the fuel price set by the considered economy and sets the unit power cost to the RO subsystem which becomes an internal power price.
- The reference design of the RO desalter has water product 489 ppm salt, membrane surface of 596,487 ft^2 and requires 12.1 MW power (6.51 kWh/ton water product). The driving simple combined cycle requires in turn 30.1 MW fuel. Design improvement lowered product ppm to 407, increased the membrane surface to 799,970 ft^2 while lowered the power requirement to 6.71 MW power (3.61 kWh/t water product). The driving simple combined cycle lowered fuel requirement to 15.2 MW.
- For RO, the reference system main decision variables are water coefficient 0.02 lb/h ft^2psi, salt coefficient 0.0007 ft/h and pressure 1500 psia. For CC, the main decisions are pinch 25 F, condenser terminal difference 10 F, compressor efficiency 0.85, gas turbine efficiency 0.9, and steam turbine efficiency 0.85. The improved design for $100/barrel economy has these main decisions 0.035, 0.0005, 1200, 5, 4, 0.916, 0.921, 0.87 and 0.9 respectively.

2.2.6. The SCC/RO ZLD configuration of 10 migd

- The configuration is similar to Fig. 5 but the reverse osmosis desalter is modified for zero liquid discharge.

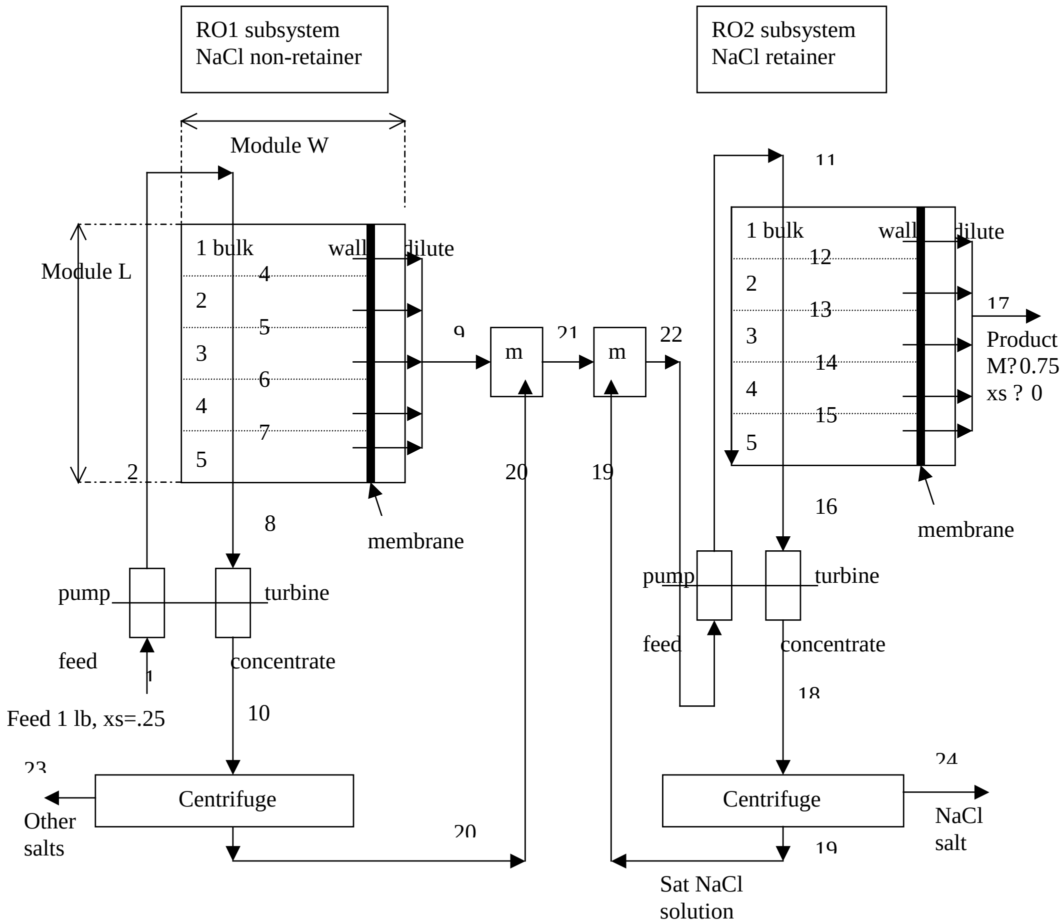

Fig. 6. A concept of RO for zero liquid discharge.

The desalter is a hypothetical two-stage desalter of zero liquid discharge.

- The RO desalter has 24 states, 10 devices and 27 decisions of which 12 are manipulated for improved designs.
- The concept of zero liquid discharge is investigated using two hypothetical stages in series. The first stage removes non sodium chloride salt species and the second removes the sodium chloride species. Feed, brine and product salt mass fractions are set at 0.035, 0.041 and 0.03 for the first stage and set at 0.26, 0.271, 0.0005 for the second assuming salt saturation limit 0.27. The result so far, is not cost effective. Power requirement increased about 8 times and so did CO_2 emission. Moreover, for the second stage, high-pressure membranes (5000 psia, probably ceramic) need to be developed.

2.2.7. The solar RO/PV configuration 0.11 usmgd product water

- The configuration represents a solar photovoltaic/reverse osmosis PV/RO system for small communities of about 1000 people. RO references are [2,4,5]. PV references are [6–8].
- The combination operates only in sun hours (default = 8 h/d)
- An assumed unit power cost minimizes the production cost of the RO subsystem. The solar subsystem minimizes the production cost of the solar subsystem given the power called by RO subsystem. The resulting unit power cost is used as the new assumed cost for the RO subsystem. The process is iterated until the assumed and computed unit power costs are equal within 0.01% deviation. This happens to require one or two iterations only.
- All minimizations are manual.
- Ten inputs (membrane water and salt permeability, applied pressure, height of brine passage, type of cell (one of 3 types), cell type standard test efficiency, cell type \$/pW, solar intensity, operating hours per year, and field de-efficiency) are varied in 9 runs. The outputs (salt ppm<500, RO surface and exergy destruction, PV surface and exergy destruction, power needed and process efficiency = theoretical work/actual work, cost of water and cost of power) are computed.

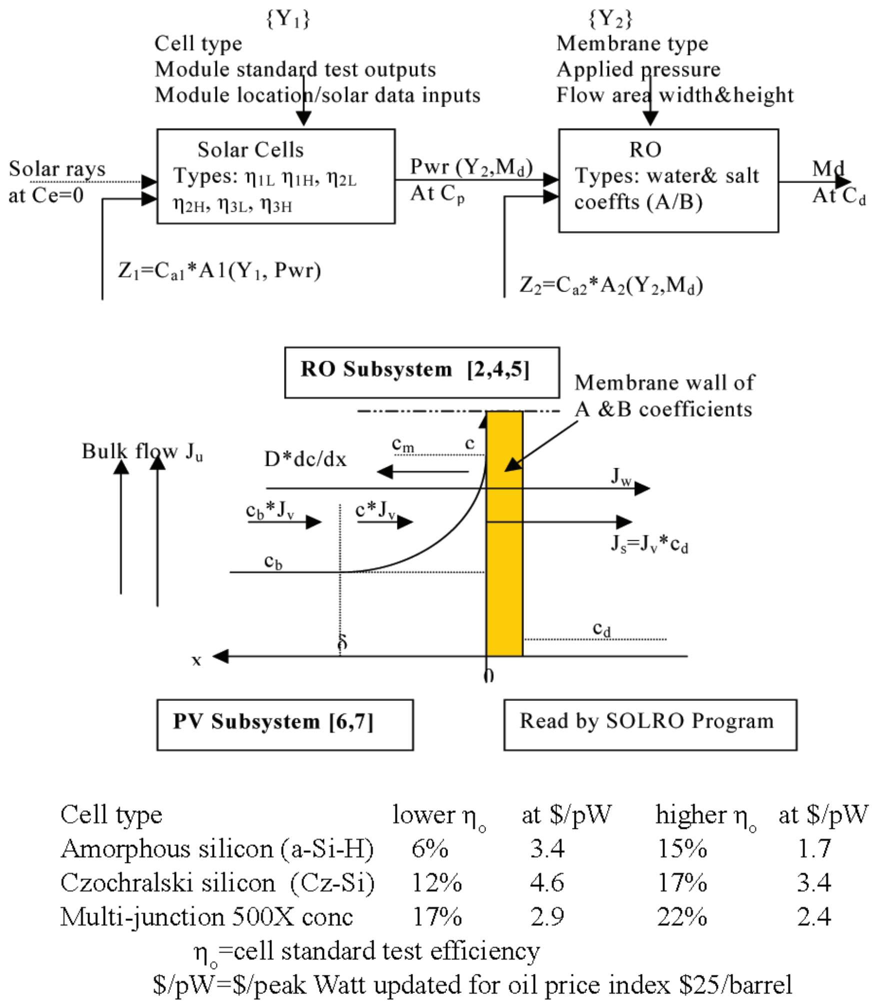

Fig. 7. The photovoltaic/reverse osmosis (PV/RO).

- As for the inputs, the first 4 runs assume 0.035 salt mass fraction seawater feed. The next 4 runs assume 0.04 seawater feed. The first 8 runs reject brine at around 0.07 salt mass fractions. The last assumes 0.01 salt mass fractions brackish water feed and rejects brine around 0.04 mass fractions. Solar intensity covered a range of 0.5–0.8 kW/m^2 but most at 0.65 kW/m^2. All runs assume operation of 365 days per year operation except one that assumes 240 days per year. The operation is limited to sunny hours only while meeting the daily water needs. All runs assume loss of cell field efficiency to 0.85 of that laboratory standard test.
- One run is competitive and 4 runs are near competitiveness
- Fig. 7a shows the area of current PV technologies [8]. Competitive PV/RO is an area between $1–2/pW and 20–30% efficiency, not far from the current area.

2.2.8. The ED/PV solar configuration 1 usmgd product water

- The configuration represents 1 usmgd solar photovoltaic/electrodialysis PV/ED system for partial recovery of irrigation drainage. ED reference is [12].
- A simple model of salt separation is used due to the lack of enough surface characteristics. The model assumes a salt separator of an overall separation efficiency connected to 7 major streams
- The PV/ED combination operates only during sun hours (default = 8 h/d)
- An assumed unit power cost minimizes the production cost of the ED subsystem. The solar subsystem minimizes the production cost of the solar subsystem given the power called for by the ED subsystem. The resulting unit power cost is used as the new assumed cost for the ED subsystem. The process is iterated until

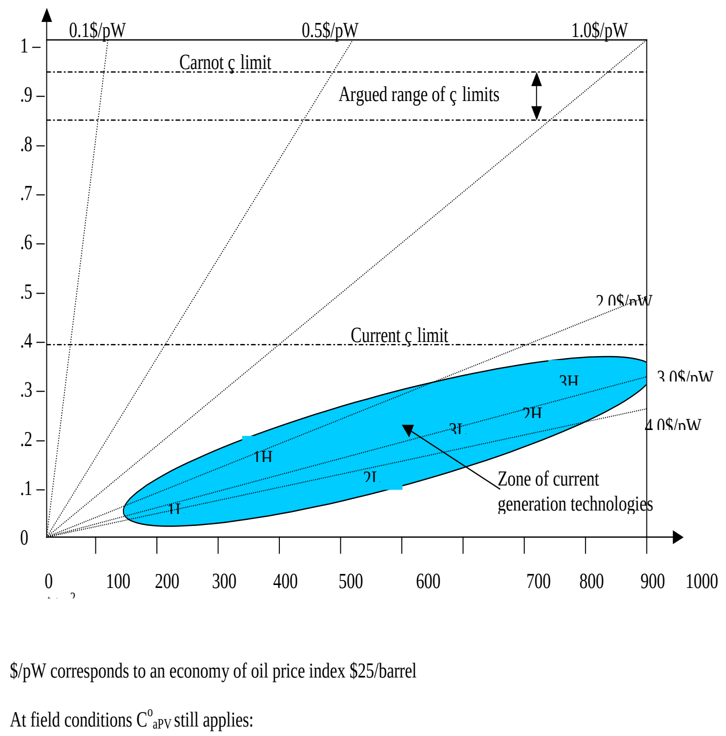

Fig. 7a. The current competitiveness of PV/RO [8].

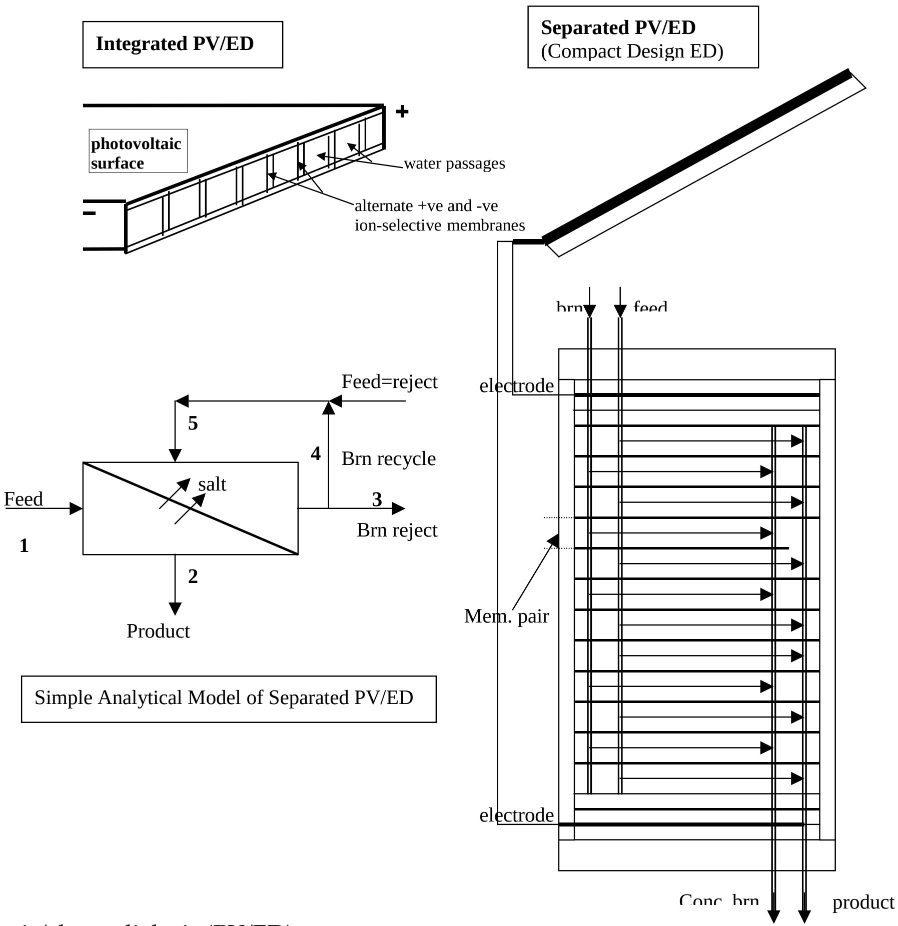

Fig. 8. The photovoltaic/electrodialysis (PV/ED).

the assumed and computed unit power costs are equal within 0.01% deviation. This happens to require one or two iterations only

- Six electrodialysis inputs (feed ppm, product ppm, ED desalting efficiency, applied volt, current density and brine recycle ratio) and the same six PV inputs are varied in ten runs. The outputs (theoretical work, ED surface and exergy destruction, PV surface and exergy destruction, power needed, pressure loss, reject brine ppm and in-brine ppm) are computed
- As for inputs, the first 6 runs assume feed of 5000 ppm salt content. One run assumes feed of 2000 ppm and two runs assume feed of 10000 ppm. Ion-exchange membrane efficiencies ranged from 0.1 to 0.6, five being at 0.3. Brine recycle ratio is 0.8 for most runs. For one run the ratio is 0.85. For three runs the ratio is set to zero. The PV inputs are the same as those of PV/RO configuration
- Three runs are competitive and three runs are near competitiveness.

2.2.9. The osmosis power systems of 10 usmgd high concentration feed

- Osmosis power [4] taps the power of a concentrated-brine stream relative to seawater.
- The power generating membrane is divided in 10 sections to compute parameter of interest on the low and the high concentration sides as well as across the membrane.
- Eight inputs (membrane water and salt permeability, x_{sh} of high concentration feed, x_{sl} of low concentration feed, x_{sj} of reject brine, height of high conc. flow passage, height of low conc. flow passage, applied $\Delta P/\Delta\Pi$) are changed in nine runs. The outputs (leaked salt, surface wall-based, surface bulk-based, output power, ideal power, efficiency = output power/ theoretical, F = high concentration salt content fall and R = low concentration salt content rise) are computed.
- As for inputs, three runs have salt permeability = 0 (no salt leakage), high concentration feed x_{sh} ranged from 0.07 to 0.25, low concentration feed x_{sl} ranged from 0.03 to 0.045. One run has x_{sl} = 0.0005 to represent a fresh water sink, x_{sj} of reject stream salt varied from 0.05 to 0.08.
- Power from conventional reject brine (x_{sh} 0.06–0.08) is not cost effective. Small power <0.5 MW is gained by large membrane surface 110 Mft^2
- For x_{sh} = 0.25 power of 20 MW is gained by a membrane surface 12 Mft^2. Only for x_{sh} = 0.1 and higher that power recovery starts to make some sense.

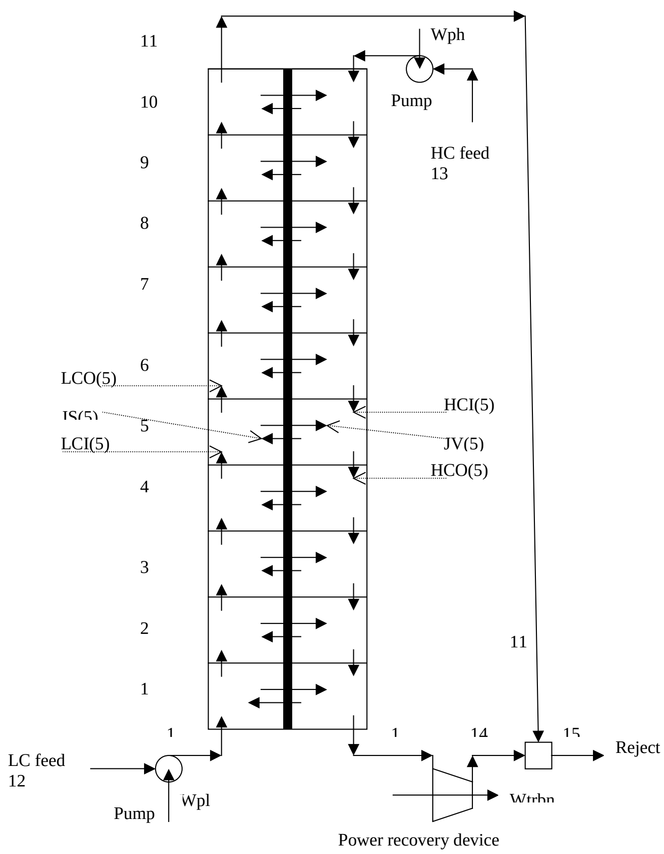

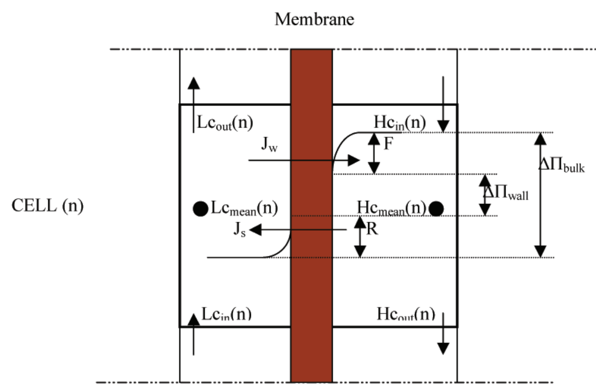

$\Delta\Pi_{bulk} = \varphi{*}R{*}T{*}(\rho_{Hcbulk}{*}XS_{Hcbulk} - \rho_{Lcbulk}{*}XS_{Lcbulk})$

$\Delta\Pi_{wall} = \Delta\Pi_{bulk}$ - F- R

F= FALL in the salt content of the high concentration fluid due to dilution by the diffusing pure water flux J_w to the high concentration side of the membrane

R= RISE in the salt content of the low concentration fluid due to the loss of diffusing pure water flux J_w to the high concentration side of the membrane and the diffusing salt flux J_s to the low concentration side. J_s=0 for membrane salt permeability coefficient B ? 0

Work recovered = A* ($\Delta\Pi_{wall}$ - ΔP) * ΔP

Theoretical work recovery W_{th} = A/4 * $\Delta\Pi^2_{bulk}$

Fig. 9. The osmosis power system.

- The salt content of water coming out from oil wells has salt content as high as 0.25. Power generation by this water when combined with seawater via membranes can be near cost effective if wells are near the sea.

2.3. The software handling the present study

Specially developed software handles the present study. The software consists of 4 programs handling the nine configurations; one handles the six natural-gas driven configurations and 3 smaller programs handle the solar driven configurations and the osmosis power tapping. The software is available on a compact disc. The disc contains the executable versions of the 4 programs along with the source code of their master programs as well as samples of library programs of properties and processes computation. The disc is available by request free of charge for anyone interested in this kind of study. The contents of the disc are self-installed in PC computers. The detailed results of each configuration on which the results of this study are based can be reproduced. Other results having reasonably different decision variables can be generated. The oil price index of the economic environment, the power load profile and the part load efficiency profile are all, accessible to the user of the software to change, and up to four night periods can be introduced for the night product.

The inputs and the corresponding outputs of the programs are presented in tables. The reason of tabulated presentation rather than graphs is the large number of decision variables. Thermodynamic decision variables are no less than 15 for any system and the thermodynamic decisions trigger design decisions and manufacture decision because of the involved design and manufacture degrees of freedom. There is no doubt that graphs are most transparent in presenting results for cases of one or two decision variables. The number of the corresponding two and three-dimensional relations explode with large number of decision variables.

3. The analyzed configurations in terms of efficiency, cost and emissions

Table 1 summarizes all analyzed cases in terms of efficiency, CO_2 emissions and unit costs of products. Table 1 is extracted from the detailed results of each configuration. The detailed results can be reproduced using the developed software for this study. The efficiency used in Table 1 for the fuel driven configurations 1–6 is the first law efficiency of the powering subsystem = work/fuel$_{hhv}$. For the solar driven configurations 7 and 8, the efficiency used is theoretical work of separation/actual work. For the osmosis configuration it is the actual work/theoretical.

3.1. Predicted competitiveness

GT/MSF results show that the case of variable power demand cogeneration takes away most of the advantage of cogeneration. This widely used cogeneration is likely to loose attractiveness in the future. The advantage is, however, maintained for the base-power-load cogeneration.

SCC results show that power-driven night products of low storing cost improves the plant load factor and raises its profitability provided the products are in short supply. The management of power generation by organized night products may gain future competitiveness.

The SCC/RO desalting systems show that the attractiveness of power driven desalting systems is likely to surpass that of distillation because of higher efficiency, lower emissions and lower product cost. The SCC/VC desalting systems come second to SCC/RO. The lower operation pressure and the higher bio-fouling resistance are advantages but the handling of large specific volumes is a disadvantage. The development of strong light material for high-speed low-pressure-ratio compressors or the development of scale-free VC operation at atmospheric pressure, reduce the disadvantage as well as the gap between the product cost by RO and VC. For example if compressor operates scale-free at 212 F (atmospheric pressure) instead of 120 F, compressor capacity would increase 15 times and its cost would be reduced about 15%. If the disadvantage is reduced, the power driven VC will gain also future attractiveness particularly for zero liquid discharge desalination. The PV/RO configuration has zero CO_2 emission and zero fossil fuel consumption but does not avoid dumping concentrated brine in the physical environment. Its future attractiveness is on the rise. The PV/ED system comes second to PV/RO if it gains sufficient development The osmosis system for power production is just a possibility not a reality and requires the availability of brine near NaCl saturation limit to combine with seawater to obtain power at acceptable cost. If developed, it can be useful of getting rid of the produced water of the oil fields located near a sea while recovering power.

4. Recommended research directions

4.1. Avoiding CO_2 emissions

- Desalination systems driven by renewable energy sources, particularly solar, are the answer if CO_2 emission is to be avoided.
- Competitiveness requires high efficiency desalting systems and solar conversion systems. RO is in the lead for high efficiency particularly for seawater. ED can be in the lead for lower salt content sources. Photovoltaic is in the lead for higher efficiency conversion to power.
- Competitiveness is raised by:
  - RO of higher water and lower salt permeability and lower cost per unit surface
  - ED of higher current density and lower electric resistance and lower cost per unit surface

Table 1
Efficiency, CO_2 emission and products costs of the analyzed systems

	Efficiency		Emission (t/h)		Night prd ($/t)	Night prd ($/t)	Wtr ($/t)	Pwr ($.kWh)	Wtr ($/t)	Pwr ($/kWh)
System	$25/brl	$100	$25/brl	$100	$25/brl	$100	$25/brl	$25	$100/brl	$100
1) GT/MSF 100 MW										
Design	0.286		62.4 (12.7 by wtr)				1.062	0.038	3.071	0.1325
Variable pwr oprn										
Without night prd	0.193		63.95				1.062	0.057	3.071	0.192
With night RO wtr	0.267		64.0		0.429	1.082	1.062	0.043	3.071	0.137
Improved design	0.296	0.327	60.8	55.0			1.094	0.037	3.027	0,1216
Variable pwr oprn										
Without night prd	0.2	0.22	61.7	55.0			1.094	0.055	3,026	0.179
With night RO wtr	0.276	0.305	61.8	56.0	.422	1.139	1.094	0.041	3.026	0.129
2) SCC 100 MW										
Design	0.402		44.7					0.036		0.122
Variable load oprn										
Without nightt prd	0.272		45.5					0.056		0.186
With RO wtr prd	0.375		45.5		0.375	1.076		0.046		0.146
With H_2 and O_2 prds	0.188		46.1		557	1990		0.072		0.252
Improved design	0.405	0.440	44.4	40.9				0.035		0.114
Variable load oprn										
Without night prd	0.272	0.297	45.1	41.6				0.054		0.174
With night RO wtr	0.376	0.416	45.2	41.0	0.374	0.971		0.044		0.137
With nightH_2 and O_2	0.189	0.205	45.7	42.1	553	1829		0.07		0.234
3) SCC/RO 10 migd										
Design	0.402	0.402	5.54	5.54			0.604	0.036	1.546	0.122
Improved design	0.404	0.439	2.98	2.745			0.56	0.035	1.226	0.114
4) SCC/RO zld 10 migd										
Design	0.402	0.402	49.5	49.5			2.147	0.036	7.2	0.112
Improved design	0.404	0.439	49.1	45.3			2.065	0.034	6.74	0.114
5) SCC/VC 10 migd										
Design	0.402	0.402	20.6	20.6			1.113	0.036	3.436	0.122
Improved design	0.405	0.439	8.46	7.8			0.949	0.035	2.346	0.114
6) SCC/VC zld 10 migd										
Design	0.402	0.402	46.04	46.04			3.024	0.036	7.151	0.11
Improved design	0.405	0.439	32.0	28.3			2.667	0.035	5.237	0.10
7) PV/RO 0.11 Usmgd										
Range of values computed	0.33–0.14		0.0				1.88–0.409	0.3–0.087	3.765–0.938	0.6–0.175
Competitive value	0.33						0.409	0.087	0.938	0.175
8) PV/EL 1 Usmgd										
Range of values computed	0.40–0.128		0.0				0.365–0.012	0.301–0.082	0.93–0.024	0.6–0.165
Competitive value	0.3						0.12	0.082	0.024	0.165
9) Osmosis 10 USmgd										
Range of values computed	0.16–0.017		0.0					27.8–0.178		55.7–0.357
Competitive value	0.16							0.178		0.357

   - PV solar cells of higher standard test efficiency and higher field efficiency and lower cost per unit surface.

4.2. Reducing CO_2 emissions

- If fossil fuels have to be used, the answers to lower CO_2 emissions are higher efficiency energy conversion devices and/or producing more products for the same emissions.
- Competitiveness is raised by
   - Cogeneration of power and desalted water by base-load power plants only.
   - Producing night low-storing-cost products to improve the load factors of power plants and of variable load (non-base load) cogeneration plants.

4.3. Avoiding dumping rejected brine by zero liquid discharge

- Adequate understanding of the feed saturation limits, their sequence, their dynamics of salt release and the separation of their solids are essential. Basic research is required.
- RO membranes for zero liquid discharge need to be developed.
   - Membranes should be designed to discriminate between salt species with respect to their solubility limits. Ideally two types are needed. One membrane retains all species except sodium chloride and one retains sodium chloride and stands pressures as high as 5000 psia.
   - A doping method for longer super-saturation time is needed to avoid the clogging of membrane passages.
- Vapor compression for zero liquid discharge may be easier to develop than membranes but the problem of handling vapor of large specific volume needs to be solved.
   - Using more than one VC in series helps to manage the large vapor volume.
   - Because several compressors may be needed, a compressor should be cheap while made of a strong light-weight composite to run efficiently at the desired high speed with less stresses.

5. Conclusions

- Solar desalination of conventional concentration ratios has a high potential to replace fossil fuel and avoids its CO_2 emission for the production of desalted water. Supporting research to improve photovoltaic conversion efficiency and the driven desalting efficiency is worthwhile. Reverse osmosis and electrodialysis are in the lead for higher desalting efficiency.
- Zero liquid discharge desalination to avoid the harm of dumping rejected brine is far from being cost effective. Further research is needed.
- Reverse osmosis driven by a simple combined cycle to produce water only has the lowest CO_2 emission because of lowest power requirement. RO driven by high-firing blade-cooled combined cycle reduces further CO_2 emission.
- Power plants and cogeneration plants that burn fossil fuel and operate under variable power demand can benefit from power-driven night products of low storage cost in short supply. Night products improve the plant load factor, produce more products for the same CO_2 emission and raise profitability.
- Raising the efficiencies of conventional energy conversion devices and reducing their costs have their limits in meeting the challenge of rising fuel prices and rising CO_2 emission. The advancement of thin film technologies seems to break these limits.

Abbreviations

GT/MSF — Gas turbine/ Multi-stage flash distillation cogeneration system
SCC — Simple combined cycle
VC — Vapor compression distiller
RO — Reverse osmosis desalter
EL — Water electrolysis system
ED — Electro-dialysis desalter
PV — Photovoltaic solar cells
ZLD — Zero liquid discharge

Symbols used by the software

A — Membrane water permeability coefficient, lb/h.ft^2.psi or m/h.bar
Surface area
A_{min} — Surface area minimized by design degrees of freedom, ft^2 (m^2).
B — Membrane salt permeation coefficient, ft/h or m/h
C_a — Cost per unit characterizing surface
C_{aRO} — RO cost per unit membrane surface
C_{aPV} — Solar-cells module cost per unit surface
C^o_{aPV} — of standard test conditions
Ca_{ED} — Cost per unit surface area of ion exchange electrodialysis membranes
C_F — Fuel price per kWh higher heating value
C_f — Fuel price per kWh exergy
C_{wtr} — Production cost per unit product, \$/m^3
C_{pwr} — Unit power cost, \$/kWh
Cap — Capital cost, Cap + added capital
C_z — Capital recovery rate \$/\$.y
C_{zM} — for membranes
C_{zRO} — for the rest of RO devices
C_{zPV} — for solar
c_d — Unit cost of exergy destruction, \$/kWh
c_{da} — System average
c — Salt concentration per unit volume, lb/ft^3 or kg/m^3

c_b – of bulk
c_m – of high-press-side membrane wall
c_d – of diluted product
d — Diameter or equivalent diameter, ft
D — Diffusion coefficient m^2/s
— Dissipation kW (exergy destruction rate)
E — Exergy
E^s — of system
E^f — of flow
EFR — Efficiency ratio = (eff. at allowed lowest load fraction) / (design eff.)
f — Friction factor
F — Fuel
Fpenalty — for fuel penalty
Fidealc — for fuel of ideal control
Npfuel — for fuel of night product
Frefired — for fuel of refiring
F_{ms} — PV cost multiplier accounting for the added cost from module to system
H — Enthalpy, height of flow passage, inch or mm
H_b — of RO membrane feed-side
H_d — of its product low-press-side
H_{hc} — of osmosis high concentration side
H_{lc} — of its low concentration side
h_m — RO mass transfer coefficient, ft/h or m/h
hhv — Fuel higher heating value
J — Objective function, \$/h, mass flux, lb/h.ft^2 or kg/h.m^2
J_w — of pure water
J_s — of salt
J_v — Volume flux, ft/h or m/h
J_u — Bulk flux
LF — Power load factor
mgd — million gallon per day, migpd — Imperial gallons, usmgd — American gallons
M_d — PV/RO water product rate, usmgd, m^3/d
N — Dimensionless number
N_V — Velocity/geometry number
N_M — Membrane number (Eq. 4.24 [2])
OP — Variable load operation
Op_{pen} — Operation cost penalty
P — Applied pressure, psia or bar
P_o — Dead state pressure
Pw — Power, kW
Pload — Power required
Pdlvrd — Power delivered
Pzn — RO concentration polarization ratio x_{sm}/x_{sb} (salt at membrane wall/bulk)
R_{eff} — The ratio of PV expected solar cells field efficiency to standard-test-conditions top cell efficiency η/η^o
R — Universal constant, resources
R_{make} — Making resources of a device
$R_{operate}$ — Operating resources of a device
R_{sol} — The ratio of design solar intensity to the standard test intensity sol/sol^o
S — Entropy
S_{RO} — RO membrane surface, m^2
S_{PV} — Solar cells surface, m^2
S^o_{PV} — of standard test conditions
Sol — Design solar intensity, kW/m^2
Sol^o — of standard test conditions (1 kW/m^2=1 sun)
T — Temperature
T_o — Dead state temperature
V — Device decision variables
$V_{efficiency}$ — Thermodynamic
V_{Design} — Design
$V_{Manufacture}$ — Manufacture
X — Dependent variable, V_{duty} for a device
x_s — Salt mass fraction
x_{sf} — of feed
x_{sj} — of reject brine
x_{sm} — at membrane wall
x_{sb} — of bulk flow
x_{sd} — of product water
Y — Decision variable
Z — Capital cost, \$
Z_{RO} — for RO subsystem
Z_{PV} — for PV module
Z_{PVS} — for solar subsystem
Z_{VC} — for VC subsystem
Z_{ED} — for electrodialysis subsystem
Z_{GT} — gas turbine subsystem
Z_{MSF} — Multistage flash distillation subsystem
$\underline{Z}$ — Capital cost rate

Greek

δ — Concentration boundary layer thickness, μm (10^{-6} m)
ΔP_h — Pressure loss psi (or kPa), high-pressure-side of RO membrane
$\Delta\Pi$ — Osmotic pressure difference
ϕ — Departure from ideal solution, 1 for ideal solution
ϕ_P — Of RO applied pressure
η — Efficiency
η_{RO} — Separation process
η_{PV} — Solar-to-power conversion
η^o_{PV} — Of standard test conditions
η_{pmp} — Adiabatic efficiency of pressurizing pump
η_{trb} — Adiabatic efficiency of work recovery turbine or device
ρ — Density
μ — Viscosity, chemical potential
μ_{co} — of species at dead state P_o and T_o

References

[1] Y.M. El-Sayed, The Thermoeconomics of Energy Conversions, Elsevier, UK, 2003.
[2] Y.M. El-Sayed, The rising potential of competitive solar desalination, Desalination, 216 (2007) 314–324.
[3] A.M. El-Nashar, Validating the simulation program “Soldes”

with actual performance data from an operating solar desalination plant, Proc. IDA World Congress on Desalination and Water Reuse, Madrid, Spain, October 6–9, 1997, 1 (1997) 107–142.
[4] M. Mulder, Basic Principles of Membrane Technology, Kluwer Academic Publishers, 2003.
[5] R.W. Baker, Membrane Technology and Applications, Wiley, New York, 2004.
[6] Y.V. Pleskov; Solar Energy Conversion: A photoelectrochemical Approach, Springer-Verlag, 1990, 163 p.
[7] A. Luque and S. Hegedus, eds., Handbook of Photovoltaic Science and Engineering, Wiley, New York, 2003.
[8] M.A. Green, Third Generation of Photovoltaics, Advanced Solar Energy Conversion, Springer-Verlag, 2003.
[9] R. Reid, J. Pruasnitz and B. Poling, The Properties of Gases and Liquids, 4th ed., McGraw Hill, 1989.
[10] Van Wylen and Sonntag, Fundamentals of Classical Thermodynamics, Wiley, 1996.
[11] A. Echeverria, Desalination plant in Tenerife, San Loranzo Valley, IDA World Congress on Desalination and Water Reuse, Madrid, Spain, October 6–9, 1997, 2 (1997) 675–694.
[12] M. Torres del Corral, M.P. del Pino, M.G. Lodos and M. Rodrigous, Physico-chemical and electrodialysis reversal treatment to reclaim wastewater from a sewage treatment plant, Proc. IDA World Congress on Desalination and Water Reuse, Madrid, Spain, October 6–9, 1997, 2 (1997) 695–711.
[13] K. Maloney and R. Dopp, Highly Efficient Hydrogen Generation via Water Electrolysis Using Nanometal Electrodes, Energy Research Laboratory, Quantum Sphere Inc., Santa Anna, CA, USA.
[14] A Richer Enterprise, Report on the Commercial Electrolytic Production of Hydrogen, Geneva, NY.
[15] Y.M. El-Sayed, Desirable enforcements to optimal system design, ECOS 2006, The 19th International Conference on Efficiency, Cost, Optimization, Simulation and Environmental Impact of Energy Systems, Aghia Pelagia, Crete, Greece, July 12–14, 2006, 1 (2006) 483–492.